HHS Public Access

Author manuscript

J Thorac Cardiovasc Surg. Author manuscript; available in PMC 2017 October 01.

Published in final edited form as:

J Thorac Cardiovasc Surg. 2016 October ; 152(4): 1059–1070.e2. doi:10.1016/j.jtcvs.2016.06.017.

Disruption of Desmin-Mitochondrial Architecture in Patients with Regurgitant Mitral Valves and Preserved Ventricular Function

Mustafa I Ahmed, MD[#b], **Jason L Guichard, MD, PhD**[#b], **Rajasekaran Namakkal Soorappan, PhD**[c], **Shama Ahmad, PhD**[d], **Nithya Mariappan, PhD**[d], **Silvio Litovsky, MD**[d], **Himanshu Gupta, MD**[a,b], **Steven G Lloyd, MD**[a,b], **Thomas S Denney, PhD**[e], **Pamela Cox Powell, MS**[a], **Inmaculada Aban, PhD**[f], **James Collawn, PhD**[g], **James E Davies, MD**[a,h], **David C McGiffin, MD**[i], and **Louis J Dell'Italia, MD**[a,b]

[a] Department of Veterans Affairs Medical Center, Birmingham (UAB), Alabama, USA

[b] Department of Medicine, Division of Cardiovascular Disease, UAB

[c] Department of Pathology, UAB

[d] Department of Anesthesiology& Perioperative Medicine, UAB

[e] Auburn University School of Engineering, Auburn, Alabama, USA

[f] Department of Biostatistics, UAB

[g] Department of Cell, Developmental, and Integrative Biology, UAB

[h] Department of Surgery, Division of Thoracic and Cardiovascular Surgery, UAB

[i] The Alfred Hospital and Monash University, Melbourne, Australia

[#] These authors contributed equally to this work.

Abstract

Objective—Recent studies have demonstrated improved outcomes in patients receiving early surgery for degenerative mitral valvular regurgitation (MR) rather than adhering to conventional guidelines for surgical intervention. However, studies providing a mechanistic basis for these findings are limited.

Corresponding author at: Louis J Dell'Italia, MD, Associate Chief of Staff for Research, Birmingham VA Medical Center, 700 South 19th Street, Birmingham, AL 35233, Telephone: (205) 558-4747, Fax: (205)-933-4471, louis.dellitalia@va.gov.

There are no conflicts of interest.

Central Message: Chronic cardiomyocyte oxidative stress and disruption of the desmin cytoskeleton may explain post-operative LV functional decline in patients with well preserved LV function and adherence to conventional guidelines.

Perspective Statement: Recent studies report improved outcomes in patients receiving early surgery for degenerative mitral regurgitation. Severe cardiomyocyte oxidative stress and desmin and mitochondrial disruption in patients with isolated mitral regurgitation and LVEF>60% may underpin the decrement in LV systolic function post valve repair and further supports the move toward earlier surgical intervention.

Central Figure legend: Disruption of the normal (**A**) desmin pattern in MR (**B**) may underpin decrease in LV function after surgery.

Methods—Left ventricular (LV) myocardium from 22 patients undergoing mitral valve repair for Class I indications was evaluated for desmin, the voltage-dependent anion channel, αβ-crystallin, and α, β unsaturated aldehyde 4-hydroxynonelal by fluorescence microscopy and in 6 normal control LV autopsy specimens. Cardiomyocyte ultrastructure was examined by transmission electron microscopy. Magnetic resonance imaging with tissue tagging was performed in 55 normal subjects and 22 MR patients pre- and 6 months post-mitral valve repair.

Results—LV end-diastolic volume was 1.5-fold ($p<0.0001$) higher and LV mass to volume ratio was lower in MR ($p=0.004$) vs. normal and improvement six months after mitral valve surgery. However, LV ejection fraction decreased from 65 ± 7 to 52 ± 9% ($p<0.0001$) and LV circumferential ($p<0.0001$) and longitudinal strain decreased significantly below normal values ($p=0.002$) post-surgery. MR hearts had a 53% decrease in desmin ($p<0.0001$) and a 2.6-fold increase in desmin aggregates ($p<0.0001$) vs. normal along with significant, intense perinuclear staining of α, β unsaturated aldehyde 4-hydroxynonelal in areas of mitochondrial breakdown and clustering. Transmission electron microscopy demonstrated numerous electron dense deposits, myofibrillar loss, Z-line abnormalities and extensive granulofilamentous debris identified as desmin positive by immunogold transmission electron microscopy.

Conclusion—Despite well-preserved preoperative LV ejection fraction, severe oxidative stress and disruption of cardiomyocyte desmin-mitochondrial sarcomeric architecture may explain post-operative LV functional decline and further supports the move toward earlier surgical intervention.

Keywords

heart failure; mitochondria; cardiomyocyte; mitral regurgitation

Introduction

Isolated/primary mitral regurgitation (MR) is a very common heart valve disease in the US. An estimated 2-2.5 million people in the US are affected by moderate to severe mitral valve disease characterized by a myxomatous degeneration of the mitral valve and progressive dilatation of the left ventricular (LV) chamber that leads to heart failure. With population growth and aging this number is expected to double by 2030 (1). Studies in asymptomatic patients with moderate to severe MR with LVEF > 60% and LVES dimension < 40 mm have shown that 30% develop symptoms of heart failure or LV dysfunction over two years with the majority progressing to these end points and the need for surgery over eight years (2-4).

Since there is no effective medical therapy for asymptomatic patients with isolated MR, the latest American College of Cardiology/American Heart Association guidelines recommend surgery as a Class I indication for moderate to severe MR in patients who are symptomatic or have progressive LV dysfunction defined by guidelines of LV ejection fraction (EF) < 60% or LV end-systolic dimension (ESD) ≥ 4.0 cm (5). In the absence of Class I indications, asymptomatic patients with LVEF > 60% and LV end- systolic diameter (LVESD) < 40 mm are only offered early repair as a Class IIa recommendation in whom the likelihood of a successful and durable repair without residual MR is greater than 95% with an expected mortality rate of less than 1% when performed at a Heart Valve Center of Excellence. The discretionary aspect of this recommendation is now being questioned based on recent studies

that report improved survival and decreased heart failure in patients undergoing early surgery before reaching Class I guidelines (6-8).

It is important to note that the majority of guidelines pertaining to timing of surgery in MR were determined in previous studies of postoperative survival, but with less assessment of postoperative LV function (5). In addition, LV systolic dysfunction assessed by echocardiography is often underestimated in patients with severe MR due to an increase in preload combined with the ejection into the low pressure left atrium. Thus, it is not surprising that adhering to general guidelines has uncovered a subset of patients who do not have an optimal outcome using the triggers of end-systolic dimension and LVEF. In a recent study from Quintana and coworkers (8) there was early postoperative LV impairment in 20% of a homogeneous population of 1,705 patients with severe degenerative MR and LVEF > 60%. As a result of this and other similar analyses, there is now a mounting objective calling for earlier surgical intervention to provide not only better postoperative survival, but also to maintain LV function.

In support of a move toward earlier surgery, we have previously demonstrated increased cardiomyocyte oxidative stress and myofibrillar degeneration in patients who have moderate to severe MR and LVEF > 60% that decreases significantly after mitral valve repair (9). The purpose of the current investigation is to report further cardiomyocyte ultrastructural damage in patients with well preserved LV systolic function. Recent studies in ours and other laboratories have demonstrated severe disruption and breakdown of desmin in an animal model of primary volume overload and in patients with dilated heart failure, similar to the desmin changes reported in genetic defects in the desmin gene. Here we test the hypothesis that patients with isolated MR and well preserved LV systolic function have extensive breakdown of the major intermediate filament desmin in addition to loss of mitochondrial damage and disarray in the sarcomeric units. The results of this study may provide a potential mechanism for the decline in LV function post-mitral valve repair and a cogent foundation for earlier surgical intervention.

Methods

Study subjects

The study protocol was approved by the University of Alabama at Birmingham Institutional Review Board and informed consent was obtained from all MR patients and control subjects. The study is divided in two parts: the clinical comparison of the study group (22 MR patients) with a control group (55 volunteers) and the immunohistochemical comparison (22 specimens from MR patients) with LV specimens from six autopsies. Twenty-two patients (mean age 57 ± 12, range 34–80) with severe isolated MR secondary to degenerative mitral valve disease were referred for corrective mitral valve surgery. Severe MR was documented on echocardiogram/Doppler studies and cine-magnetic resonance imaging (MRI) in all cases. All patients had cardiac catheterization prior to surgery. Patients with obstructive coronary artery disease (> 50% stenosis), aortic valve disease, or concomitant mitral stenosis were excluded. This patient population was selected from a consecutive series of patients recruited under the funding of our NIH Specialized Center for Clinically Oriented Research between the time of June 2005 and July of 2010

(P50HL077100) (n = 60), with surgery performed by Dr. David McGiffin. Of this number, 22 patients were selected based on the availability of remaining biopsy sample for desmin analysis and the presence of more than 3 high powered fields of longitudinally directed cardiomyocytes for adequate desmin analysis and quantification. All patients had degenerative mitral valve disease documented by echocardiography manifested by thickening and prolapse of the mitral valve and by the surgeon's description at operation. All patients had Carpentier II mitral valve disease.

Patients underwent magnetic resonance imaging (MRI) with tissue tagging prior to and six months after mitral valve repair. All MRI studies were obtained within one month of surgery and 6 months after surgery. Only 3 patients did not have a 6 month study. MRI was also performed in 55 control volunteers (age 45 ± 14, median 45, range 20–70 years). These subjects were recruited for the study and were included if they did not have a history of cardiovascular disease and smoking, and were not taking any type of cardiovascular medication, including statins. All control subjects signed an informed consent form approved by the UAB IRB.

Magnetic resonance imaging

MRI was performed on a 1.5-T scanner (Signa GE, Milwaukee, Wisconsin) optimized for cardiac application and LV volumes were computed from summated serial short axis slices as previously described in our laboratory (2,9,10). Tagged magnetic resonance images were acquired on the same scanner with repetition/echo times of 8/44 ms, and tag spacing of 7 mm. Three-dimensional LV strain was measured from tagged images at end-systole, which was defined by visual inspection of the image data as the time frame with maximum contraction. Strain computations were conducted using an in-house software package as previously described by our laboratory (9,10). Strains were computed at midwall segments as defined by Cerqueira et al. (11).

Surgical Methods

At surgery, LV myocardial tissue was taken from the endocardium of the LV lateral posterior wall at the level of the tips of the papillary muscles in all patients. The biopsy was taken as soon as left atrium was opened which was immediately after cardioplegic arrest, in all cases no longer than five minutes after cardiopulmonary arrest. Mitral valve repair was performed through median sternotomy and standard hypothermic cardiopulmonary bypass and cold blood cardioplegia. A variety of methods were used to repair the mitral valve including leaflet resection, chordal replacement or a combination of each. All patients had implantation of a flexible annuloplasty band. Repair was assessed by intraoperative transesophageal echocardiography.

Immunohistochemistry

Control LV myocardial specimens were obtained at time of autopsy in patients with no evidence of myocardial or valvular disease. The specimens were obtained from: 31 yo male drug abuse, 45 yo male motor vehicle accident, 24 yo male drug abuse, 28 yo male drug abuse, 34 yo male schizophrenic, 47 yo female with chest pain for a week. Patient biopsies were fixed, paraffin-embedded and processed for immunohistochemistry as previously

described (9). Sections were incubated with antibodies: VDAC (Abcam #ab14734; 1:500), alpha β-crystallin (Enzo # ADI-SPA-223; 1:100), desmin (Abcam #ab15200 or #ab6322; 1:200), α, β unsaturated aldehyde 4-hydroxynonelal (4-HNE) (Millipore #393207; 1:200), and catalase (Millipore #219010; 1:200). Alexa Fluor 488- and 594-conjugated secondary antibodies (1:700, Life Technologies) with appropriate host combinations were used to stain for visualization. Nuclei were labeled with DAPI (1.5μg/ml, Vector Laboratories #H-1500). Image acquisition for desmin and 4-HNE were performed on a Leica DM6000 epifluorescence microscope with Simple-PCI Imaging software (Compix, Inc). Pixel intensity was analyzed by measuring the intensity (mean red, mean green) of the fields.

Transmission electron microscopy (TEM) of LV tissue

Eight of the 22 patients had TEM analysis. Patient biopsies were fixed in 2.5% Glutaraldehyde/Sorensen's Phosphate Buffer (Electron Microscopy Sciences #15980) overnight at 4°C as previously described by our laboratory (9). Sections were viewed in a Philips 201 TEM (FEI Co.) by EMLabs Inc (Birmingham, AL). Immuno–electron microscopy (EM) was used to detect desmin at ultrastructural level as described by Wang et al., (12). The human heart biopsy pieces were submerged in 0.1% glutaraldehyde/2% paraformaldehyde in cardioplegic buffer (5% dextrose, 30 mmol/L KCl in PBS), further fixed in the same fixative in cacodylate buffer, incubated in 0.1 mol/L glycine/PBS, dehydrated in series of N, N-dimethyl formamide, and embedded in LRWhite resin. Ultrathin (90 nm) sections (10-12) were picked up on nickel grids (3 mm) and dried. Before immunolabeling grids were rinsed in PBS and blocked for 1.5 h with 1% BSA, 0.1% cold water fish skin gelatin, and 1% Tween 20 in PBS. Grids were then incubated desmin antibody (Abcam #ab15200), diluted 1:25 with 1% BSA/PBS first for 2 h at room temperature (RT) and then overnight at 4°C. The grids were rinsed with P BS, blocked and incubated (RT, 2h) with goat anti-rabbit IgG tagged with colloidal gold (10-nm particle size, diluted 1:50 with 1% BSA/PBS) (Aurion/Electron Microscopy Sciences). Sections were postfixed and counterstained with uranyl acetate and viewed on a FEI-Tecnai T12 Spirit 20 electron microscope at 120 kv.

Statistical Analysis

Data are presented as mean ± SD or counts (%). Age and gender were compared between 22 MR and 55 normal controls using non-paired t-test and chi-squared test, respectively. Intensity measurements from normal and MR LV for desmin and 4-HNE were compared with an exact Wilcoxon 2-sample test. To enable pairwise comparisons of the 3 groups of interest (normal subjects, baseline MR, and 6-month post-MV repair) in one model, we defined a group variable with these 3 categories. In modeling the clinical characteristics (BSA, heart rate, SBP, DBP) and MRI functional data (LVEDD, LVESD, LVEDV, LVESV, LVEF, LVED mass/volume, LVED sphericity index, LV circumferential and longitudinal strains), we fitted a generalized linear model separately for each outcome with group as the main variable of interest using generalized estimating equations and assuming a gamma distribution. Analyses were done using the GENDMOD procedure in SAS version 9.3 software (SAS Institute, Cary, North Carolina) using the REPEATED statement with an exchangeable working correlation structure to account for the correlation between pre- and post-surgery readings. We added age as covariate to address the imbalance between MR and

normal controls in the MRI analyses. To avoid inflating the probability of a type I error due to testing these 9 primary MRI paramters, the Bonferroni-Holm step-down method was used to adjust the significance level in the determination of the significance of the group main effects maintaining a family-wise significance level of 0.05. Once the group effect is deemed significant for a given MRI parameter, we perform pairwise comparisons (pre vs post, pre vs. normal, and post vs. normal) using a cut off of $p<0.0167(=0.05/3)$.

Results

Patient Characteristics and MRI Parameters (Table 1 and Supplementary Table 2)

Body surface area, heart rate, or blood pressure did not differ among control and pre- and post-mitral valve repair groups. All patients were referred to the UAB Cardiovascular Surgery Clinic and had either tranesophageal (4) or transthoracic (18) LVESD ≤ 4.0 cm or LVEF > 55% by visual inspection. Mean age of control subjects was 45 ± 14 and MR patients 57 ± 12 years (p=0.0006). MR patients were New York Heart Association Class I (27%), Class II (64%) or Class III (9%). No MR patients had atrial fibrillation. LVED volume was increased > 50% in MR patients vs. controls (195 ± 50 vs. 127 ± 27 ml p<0.0001) and decreased post-mitral valve repair (152 ± 45 ml p=0.0002). LVED sphericity index (LVED length/LVED inner diameter) pre- and post-surgery (1.49 ± 0.19 and 1.58 ± 0.19 respectively) were significantly different from normal controls (1.77 ± 0.18, p <0.0001 and p=0.001 respectively) but did improve post-surgery. LVED mass to volume ratio pre-surgery (0.65 ± 0.13 g/ml) was significantly different from normal controls (0.75 ± 0.17 g/ml, p=0.0042) but did improve and did not differ from normal post-surgery (0.75 ± 0.20 g/ml, p=0.0013). Thus, there was evidence of preserved LV systolic function in the presence of adverse LV remodeling which did improve post mitral valve surgery manifested by a normalization of the LVED mass to volume ratio.

LVEF decreased from 65 ± 7 to 52 ± 9% (p<0.0001) after surgery. LVES volume was higher in MR vs. controls (67 ± 20 vs. 45 ± 14 ml, p<0.0001) and did not change significantly post-surgery. LVES dimension changed in similar directions as LV volumes. LV circumferential systolic shortening strains were significantly decreased following mitral valve repair vs. before surgery (p<0.001) and vs. normal control subjects (p<0.0001). LV longitudinal systolic shortening strains were not different from normal controls before surgery, but were decreased following MV repair vs before surgery (p=0.0013) and relative to normal control subjects (p=0.0020) (**Figure 1**). The color-coded strain map in **Figure 1** demonstrates the significant global decrease in circumferential and longitudinal strains in a representative MR patient post mitral valve repair.

Disruption of cardiomyocyte cytoskeletal-mitochondrial architecture in MR patients (Figure 2)

TEM images at 4,500X in three different representative MR patients with LVEF > 60% (**Figure 2, left panels**) demonstrate numerous clusters of small round mitochondria with complete disruption of the normal mitochondrial linear registry that is normally in close proximity to the sarcomeric myofibrils. In Patients 1 and 2 (**Figure 2**), white boxes demarcate the perinuclear areas at 4,500X and accompanying 16,000X images to the right

demonstrate large electron dense aggregates containing lipid droplets consistent with lipofuscin. There are numerous lipid droplets throughout the myocardium. In **Patient 3 (bottom panels)**, white box in the 4,500X image marks an interfibrillar area with mitochondrial breakdown and areas of granulofilamentous protein aggregates within autophagic vacuoles (**Patient 3, right panel white arrow**).

Desmin degradation in the LV of patients with isolated MR

The normal human LV has a striated registry of desmin staining in Z-discs and more intense staining at intercalated discs (**Figure 3A, arrow heads**) with VDAC staining mitochondria in a single linear registry between sarcomeres. MR hearts from two patients with LVEF > 60% (**Figure 3B and C**) demonstrate disrupted or near complete absence of desmin in some cardiomyocytes. Other areas have intense desmin staining, especially in perinuclear areas, which is consistent with desmin aggregates (**white arrows in Figure 3B and C**). There is a 50% decrease in desmin staining vs. normal hearts ($p<0.0001$) and a significant increase in desmin aggregates vs. normal ($p<0.0001$) (**Figure 3D**). There are areas of increased VDAC staining indicating focal mitochondrial clustering as seen in the TEM examples in **Figure 2**. **Figure 4** demonstrates TEM with desmin immunogold labeling in the MR heart of a patient with LVEF of 65%. There is marked disruption and degradation of the mitochondrial sarcomeric units (left panel). Box defines define areas of higher magnification (right panel) of immunogold labeling for desmin (black dots) in the areas of myofibrillar degradation near the interfibrillar disorganization of mitochondria.

Figure 5 A-C demonstrates the normal location of αβ-crystallin in the Z-disc (B) forming a striated pattern with desmin as seen in the merged image in **Figure 5C**. In MR, there is translocation of αβ-crystallin to the perinuclear regions (**Figure 5 E and H**) that co-stains with desmin especially in the perinuclear area as seen in the merged images (**Figure 5F and I**). This αβ-crystallin translocation coincides with the extensive perinuclear granulomatous debris and electron dense aggregates demonstrated in TEMs in Patients 1 and 2 in **Figure 2**. This translocation of α, β-crystallin from the Z-disc to the perinuclear area in the MR heart along with co-staining with desmin in merged images (**Figure 5F and I**) is consistent with its chaperone function of clearing desmin breakdown products. However, the extensive accumulation of both desmin and αβ-crystallin suggests a failure of clearance of cytoskeletal breakdown products.

Evidence of Excessive Oxidative Stress in MR Cardiomyocytes

One of the major causes of desmin disruption/aggregates and mitochondrial disarray is excessive oxidative stress. HNE is a very strong indicator of oxidative stress in particular lipid peroxidation that is increased two-fold ($p=0.011$) in MR hearts. Figure 6 demonstrates the significant increase in 4-HNE in three patients with LVEF > 60%. There is a strong signal in the perinuclear region that coincides with VDAC staining in Figure 3 and in TEM images of Patients 1 and 2. The co-localization of HNE and VDAC is consistent with lipid peroxidation of the membrane rich mitochondria in the cardiomyocyte. The increase in HNE is associated with a moderate increase in catalase especially in the perinuclear regions in the same MR patients in Figure 7 (B-D) compared to the normal LV (Figure 6A). The increase

in catalase has also been reported in heart failure patients in response to increased oxidative stress (13).

To address the question of generalizability of the biopsy findings to a more contemporary patient population, we include six recently studied patients in 2015-2016 under the funding of an NIH PPG (P01HL051952 - 21A1) (Supplementary Table 2). These are consecutive patients referred to Dr. Davies for surgical opinion with degenerative mitral regurgitation over a period of 5 months. All patients signed informed consent and had degenerative MR documented by echocardiography/Doppler examination and at the time of surgery. Inclusion and exclusion criteria were the same as in the main patient population and all patients had Carpentier II mitral valve disease and were within Class I echocardiographic guidelines (Supplementary Table 2). Representative TEMs in two patients demonstrate numerous electron dense particles with mitochondrial clustering and sarcomere breakdown (Supplementary Figure 1). In these same patients, there is significant degradation of desmin and accumulation of aggregates (Supplementary Figure 2, p=0.0043) with intense HNE staining.

Discussion

Our studies demonstrate breakdown of desmin and mitochondrial/sarcomeric disruption in cardiomyocytes of patients with well-preserved LV systolic function. These findings along with a decrease in LV function post-mitral surgery suggest that despite a significant decrease in LVED volume and normalization of LVED mass/volume ratio, disruption of the cardiomyocyte cytoskeletal-mitochondrial architecture may preclude an improvement in LV systolic function. Importantly, these results provide a potential mechanism for recent findings that a substantial subset of patients have unfavorable outcome despite adherence to guideline triggers and LVEF>60% prior to surgery.

In the current study we utilize immunofluorescence microscopy, TEM, and immuno-TEM to characterize the severe desmin cytoskeletal disruption in the MR hearts. It is of interest that TEM findings in our MR patients are similar to cardiac findings in patients with mutations of the desmin gene (14,15) or its main chaperone αβ-crystallin (16), as well as other cytoskeletal cardiomyopathies (17). Desmin is the predominant intermediate filament protein expressed in the heart, interacts with other structural proteins at the Z-disc, and extends from the subsarcolemmal membrane to nucleus (18). This continuous 3-dimensional cytoskeletal network maintains the close spatial relationship between the sarcomere contractile apparatus and the mitochondria and provides cellular integrity and mechanochemical signaling necessary for sarcomere growth and force transmission (18). Currently, 49 mutations have been identified in desmin gene that alter desmin filament assembly process (19) and result in disorganization of the desmin network and accumulation of desmin-containing aggregates. Transgenic mice with a missense mutation (R120G) of αβ-crystallin recapitulate the human cardiomyopathic phenotypes, with desmin disruption and formation of perinuclear αβ-crystallin aggregates and progression to a dilated cardiomyopathy by 5–7 months of age (20). Disorganization of desmin and mitochondria functional complexes with myofibrils and sarcoplasmic reticulum are present prior to the onset of cardiac and skeletal muscle failure in these animal models (17,21).

While desmin disintegration is common in various forms of genetic cardiomyopathies caused by mutations in structural proteins, our findings are unique in that the MR hearts exhibiting chronic oxidative stress have desmin breakdown and the compensatory chaperone- (α, β-crystallin) mediated protection fails to prevent progressive degradation and accumulation of desmin. In MR hearts, the extensive desmin breakdown and small clusters of mitochondria are accompanied by re-localization of α, β-crystallin from the Z disc to the perinuclear area where it accumulates along with electron dense aggregates and intense HNE staining. 4-HNE is a highly reactive α,β-unsaturated aldehyde generated by reactive oxygen species reacting with polyunsaturated fatty acids in biological membranes, in particular the inner membrane of mitochondria (22). It is of interest that the intense HNE staining is seen in the interfibrillar and perinuclear areas of abundant damaged mitochondria of the MR heart and its concentration in LV tissue has been related to severity of LV dysfunction in patients with heart failure (22). αβ-crystallin is the most abundant small heat shock protein in the heart (23) and serves as a chaperone for desmin and other proteins by preventing them from aggregating under stress conditions. In the MR hearts, the dense perinuclear staining suggests a failure to clear desmin fragments and other oxidatively modified proteins as suggested by the lipofuscin-like electron dense particles.

Desmin cleavage and the formation of desmin amyloid-like oligomers has recently been reported in failing human hearts and in hearts of dogs with dyssynchronous heart failure (24). We have reported desmin breakdown and increased cardiomyocyte oxidative stress in rats with the primary volume overload of aortocaval fistula and in isolated cardiomyocytes subjected to cyclical stretch (25). Other studies have recently shown a similar disruption and patchy loss of desmin in left ventricles of patients with ischemic cardiomyopathy that is related to the extent of LV dysfunction and poor prognosis (26,27). The relation of desmin breakdown to long-term survival and to severity of LV dysfunction in human heart failure provides compelling evidence for a non-genetic cause of desmin degradation in the pathophysiology of LV functional deterioration in human heart failure and our MR patients.

Although excessive oxidative stress is a major factor, the mechanism of desmin breakdown in the pathophysiology of MR or heart failure is multifactorial. In addition to cardiomyocyte HNE, we find an increase in catalase, which is a hydrogen peroxide scavenging enzyme that is increased in response to increased oxidative stress in failing human hearts (13). These markers of increased oxidative stress are consistent with our previous report of increased xanthine oxidase in patients with isolated MR and LVEF > 60% (9). Human isolated MR has also been associated with upregulation of TNF-alpha expression (28) and increased adrenergic drive (29,30), which are related to severity of LV dilatation and systolic dysfunction. Desmin is a major substrate for the intracellular calcium dependent protease calpain, which is activated during the high intracellular Ca^{2+} levels, achieved during ischemia/reperfusion (31,32) but also with increased TNF-alpha and excessive β-adrenergic signaling and oxidative stress (32). It is of interest that β_1-adrenergic receptor blockade improves cardiomyocyte and LV function and reverses myofibrillar degradation in dogs with isolated experimental MR (33,34), improves LV diastolic and systolic function over two years in patients with isolated MR (2), and decreases oxidative stress and HNE production in LVs of patients with heart failure (22). These findings support a link of incessant adrenergic

drive and cardiomyocyte oxidative stress to protease activation and cytoskeletal breakdown in the adverse LV remodeling of the MR heart.

In the patient with isolated MR, the 10 unit decrease in LVEF post-mitral valve surgery has in part been attributed to a LV volumetric adjustment brought about by a decrease in preload combined with correction of ejection into the low pressure left atrium. In our MR patients, circumferential and longitudinal shortening strains decrease below normal after mitral valve repair, despite normalization of the LVED mass/volume ratio, an index of wall stress. We have previously reported persistence of decreased LV shortening strains at one year, suggesting that the decrease in LV systolic function may be due to persistent cytoskeletal-myofibrillar-mitochondrial damage (18). Indeed, the recent studies demonstrating an increased incidence of heart failure and mortality in MR patients with Class I echo characteristics also suggest more severe myocardial damage as a mechanism of this outcome.

It is now well appreciated that even with strict adherence to guideline recommendations, there is a decrease in LVEF and an unacceptable incidence of heart failure after surgical repair. The severe disruption of desmin and excessive cardiomyocyte oxidative stress in our patients with well preserved LV systolic function now provide a novel mechanistic insight into the adverse LV spherical remodeling and a potential explanation for improved outcome with surgery before traditional guideline triggers. Considering the extensive mitochondrial disarray and the more chronic autophagic vacuoles and electron dense aggregates, we feel this is not a result of diastolic arrest. This contention is supported by work in the dog demonstrating preserved mitochondrial structure and sarcomeric integrity in LV endomyocardium of dogs undergoing warm or cold cardioplegia by Kamoli et al (35). However, we cannot rule out the possibility of normalization of ultrastructural derangement after repair or that the desmin changes are unrelated to the natural history of the ventricle. The major point of the current investigation is that severe ultrastructural damage is already present at the time of surgery in patients by the time symptoms have developed or guidelines have been achieved. Using a three-dimensional analysis of cine-MR in patients with degenerative MR, we (10) have demonstrated that LVES dimension belies the extensive LV spherical remodeling distal to the base of the heart, thus militating for an LVES volume rather than LVES dimension indication for surgical intervention. Further studies are needed to establish prospectively the value of LVES volume/sphericity and novel circulating biomarkers in predicting LV function following MV repair.

Supplementary Material

Refer to Web version on PubMed Central for supplementary material.

Acknowledgments

This work was supported by NHLBI and Specialized Centers of Clinically Oriented Research grant P50HL077100 (LJD) in cardiac dysfunction, by Department of Veteran Affairs for Merit Review (Grant 1CX000993-01 to LJD) and by NIH Grant P01 HL051952 (LJD) NHLBI Training Grant 5-T32-HL-072757 (JLG), and R01HL118067 (RNS).

Abbreviations

LV	Left Ventricle
LVEF	Left Ventricular Ejection Fraction
ES	End-Systolic
ED	End-Diastolic
MRI	Magnetic Resonance Imaging
MR	Mitral Regurgitation
TEM	Transmission Electron Microscopy
VO	Volume Overload
VDAC	Voltage-dependent Anion Channel
HNE	α, β unsaturated aldehyde 4-hydroxynonelal

References

1. Enriquez-Sarano M, Akins CW, Vahanian A. Mitral regurgitation. Lancet. 2009; 373:1382–94. [PubMed: 19356795]
2. Ahmed MI, Aban I, Lloyd SG, Gupta H, Howard G, Inusah S, Peri K, et al. A randomized controlled Phase IIb trial of Beta-1 receptor blockade in isolated degenerative mitral regurgitation. J Am Coll Cardiol. 2012; 60:833–38. [PubMed: 22818065]
3. Suri RM, Aviernos J-F, Dearani JA, Mahoney DW, Michelena HI, Schaff HV, Enriquez-Sarano M. Management of less-than-severe mitral regurgitation: should guidelines recommend earlier surgical intervention. Eur J Cardiovasc Surg. 2011; 40:496–502.
4. Enriquez-Sarano M, Avierinos JF, Messika-Zeitoun D, Detaint D, Capps M, Nkomo V, et al. Quantitative determinants of the outcome of asymptomatic mitral regurgitation. N Eng J Med. 2005; 352:875–83.
5. Nishimura RA, Otto CM, Bonow RO, Carabello BA, Erwin JP III, Guyton RA, et al. 2014 AHA/ACC Guideline for the management of patients with valvular heart disease: report of the American College of Cardiology/American Heart Association Task Force on Practice Guidelines. Circulation. 2014; 129:2440–92. [PubMed: 24589852]
6. Enriquez-Sarano M, Suri RM, Clavel MA, Mantovani F, Michelena HI, Pislaru S, et al. Is there an outcome penalty linked to guideline-based indications for valvular surgery? Early and long-term analysis of patients with organic mitral regurgitation. J Thorac Cardiovasc Surg. 2015; 150(1):50–8. [PubMed: 25986494]
7. Goldstone AB, Patrick WL, Cohen JE, Aribeana CN, Popat R, Woo YJ. Early surgical intervention or watchful waiting for the management of asymptomatic mitral regurgitation: a systematic review and meta-analysis. Ann Cardiothorac Surg. 2015; 4(3):220–29. [PubMed: 26309823]
8. Quintana E, Suri RM, Thalji NM, Daly RC, Dearani JA, Burkhart HM, et al. Left ventricular dysfunction after mitral valve repair-the fallacy of "normal" preoperative myocardial function. J Thorac Cardiovasc Surg. 2014; 148:2752–62. [PubMed: 25173130]
9. Ahmed M, Gladden JD, Litovsky S, Lloyd SG, Gupta H, Inusah S, et al. Myofibrillar degeneration, oxidative stress and post-surgical systolic dysfunction in patients with isolated mitral regurgitation and pre-surgical LV ejection fraction > 60%. J Am Coll Cardiol. 2010; 55:671–79. [PubMed: 20170794]
10. Schiros CG, Dell'Italia LJ, Gladden JD, Clark D 3rd, Aban I, Gupta H, et al. Magnetic resonance imaging with three-dimensional analysis reveals important left ventricular remodeling in isolated

mitral regurgitation: implications beyond dimensions. Circulation. 2012; 125:233–42. [PubMed: 22179538]

11. Cerqueira MD, Weissman NJ, Dilsizian V, Jacobs AK, Kaul S, Laskey WK, et al. Standardized myocardial segmentation and nomenclature for tomographic imaging of the heart: a statement for healthcare professionals from the Cardiac Imaging Committee of the Council on Clinical Cardiology of the American Heart Association. Circulation. 2002; 105:539–42. [PubMed: 11815441]
12. Wang X, Osinska H, Dorn GW 2nd, Nieman M, Lorenz JN, Gerdes AM, Witt S, Kimball T, Gulick J, Robbins J. Mouse model of desmin-related cardiomyopathy. Circulation. 2001; 103(19):2402–7. [PubMed: 11352891]
13. Dieterich S, Bieligk U, Beulich K, Hasenfuss G, Prestle J. Gene expression of antioxidative enzymes in the human heart. Increased expression of catalase in the end-stage failing heart. Circulation. 2000; 101:33–9. [PubMed: 10618301]
14. Schröder R, Goudeau B, Simon MC, Fischer D, Eggermann T, Clemen CS, et al. On noxious desmin: functional effects of a novel heterozygous desmin insertion mutation on the extrasarcomeric desmin cytoskeleton and mitochondria. Hum Mol Genet. 2003; 12(6):657–69. [PubMed: 12620971]
15. Bär H, Fischer D, Goudeau B, Kley RA, Clemen CS, Vicart P, et al. Pathogenic effects of a novel heterozygous R350P desmin mutation on the assembly of desmin intermediate filaments in vivo and in vitro. Hum Mol Genet. 2005; 14(10):1251–60. [PubMed: 15800015]
16. Vicart P, Caron A, Guicheney P, Li Z, Prévost MC, Faure A, et al. A missense mutation in the alphaB-crystallin chaperone gene causes a desmin-related myopathy. Nat Genet. 1998; 20(1):92–5. [PubMed: 9731540]
17. McClendon PL, Robbins J. Desmin-related cardiomyopathy: an unfolding story. Am J Physiol Heart Circ Physiol. 2011; 301:H1220–H28. [PubMed: 21784990]
18. Saks V, Guzun R, Timohhina N, Tepp K, Varikmaa M, Monge C, et al. Structure-function relationships in feedback regulation of energy fluxes in vivo in health and disease: Mitochondrial Interactosome. Biochim Biophys Act. 2010; 1797:678–97.
19. Dalakas MC, Park K-Y, Semino-Mora C, Lee HS, Sivakumar K, Goldfarb LG. Desmin myopathy, a skeletal myopathy with cardiomyopathy caused by mutation of the desmin gene. New Eng J Med. 2000; 342:770–80. [PubMed: 10717012]
20. Wang X, Osinska H, Klevitsky R, Gerdes AM, Nieman M, Lorenz J, et al. Expression of R120G-αβ-crystallin causes aberrant desmin and αβ-crystallin aggregation and cardiomyopathy in mice. Circ Res. 2001; 89:84–91. [PubMed: 11440982]
21. Milner DJ, Weitzer G, Tran D, Bradley A, Capetanaki Y. Disruption of muscle architecture and myocardial degeneration in mice lacking desmin. J Cell Biol. 1996; 134:1255–70. [PubMed: 8794866]
22. Nakamura K, Kusano K, Nakamura Y, Kakishita M, Ohta K, Nagase S, et al. Carvedilol decreases elevated oxidative stress in human failing myocardium. Circulation. 2002; 105(24):2867–71. [PubMed: 12070115]
23. Bennardini F, Wrzosek A, Chiesi M. αβ-crystallin in cardiac tissue. Association with actin and desmin filaments. Circ Res. 1992; 71:288–94. [PubMed: 1628387]
24. Agnetti G, Halperin VL, Kirk JA, Chakir K, Guo Y, Lund L, et al. Desmin modifications associate with amyloid-like oligomers deposition in heart failure. Cardiovasc Res. 2014; 102:24–34. [PubMed: 24413773]
25. Yancey D, Guichard J, Ahmed MI, Zhou L, Murphy MP, Johnson MS, et al. Cardiomyocyte Mitochondrial Oxidative Stress and Cytoskeletal Breakdown in the Heart with a Primary Volume Overload. Am J Physiol Heart Circ Physiol. 2015; 308:H651–63. [PubMed: 25599572]
26. Di Somma S, Di Benedetto MP, Salvatore G, et al. Desmin-free cardiomyocytes and myocardial dysfunction in end stage heart failure. Eur Jour Heart Fail. 2004; 6:389–98. [PubMed: 15182762]
27. Di Somma S, Marotta M, Salvatore G, Cudemo G, Cuda G, De Vivo F, et al. Changes in myocardial cytoskeletal intermediate filaments and myocyte contractile dysfunction in dilated cardiomyopathy: an in vivo study in humans. Heart. 2000; 84(6):659–67. [PubMed: 11083750]

28. Oral H, Sivasubramanian N, Dyke DB, Mehta RH, Grossman PM, Briesmiester K, et al. Myocardial proinflammatory cytokine expression and left ventricular remodeling in patients with chronic mitral regurgitation. Circulation. 2003; 107(6):831–7. [PubMed: 12591752]

29. Grossman PM, Linares OA, Supiano MA, Oral H, Mehta RH, Starling MR. Cardiac-specific norepinephrine mass transport and its relationship to left ventricular size and systolic performance. Am J Physiol Heart Circ Physiol. 2004; 287:H878–H88. [PubMed: 15072949]

30. Zheng J, Yancey D, Ahmed MI, Wei CC, Powell PC, Shanmugam M, et al. Increased Sarcolipin expression and adrenergic drive in patients with chronic isolated mitral regurgitation. Circulation Heart Failure. 2014; 7:194–02. [PubMed: 24297688]

31. Pappa Z, van der Veldenb J, Stienen GMM. Calpain-I induced alterations in the cytoskeletal structure and impaired mechanical properties of single myocytes of rat heart. Cardiovasc Res. 2000; 45:981–93. [PubMed: 10728424]

32. Goll DE, Thompson VF, Li H, Wei W, Cong J. The calpain system. Physiol Rev. 2003; 83:731–801. [PubMed: 12843408]

33. Pat B, Killingsworth C, Denney T, Zheng J, Powell P, Tillson M, et al. Dissociation between cardiomyocyte function and remodeling with beta-adrenergic receptor blockade in isolated canine mitral regurgitation. Am J Physiol Heart Circ Physiol. 2008; 295(6):H2321–H37. [PubMed: 18849331]

34. Tsutsui H, Spinale FG, Nagatsu M, Schmid PG, Ishihara K, DeFreyte G, et al. Effects of chronic beta-adrenergic blockade on the left ventricular and cardiocyte abnormalities of chronic canine mitral regurgitation. J Clin Invest. 1994; 93:2639–48. [PubMed: 7911128]

35. Kamlot A, Bellows SD, Simkhovich BZ, Hale SL, Aoki A, Kloner RA, Kay GL. Is warm retrograde blood cardioplegia better than cold for myocardial protection? Ann Thorac Surg. 1997; 63:98–104. [PubMed: 8993249]

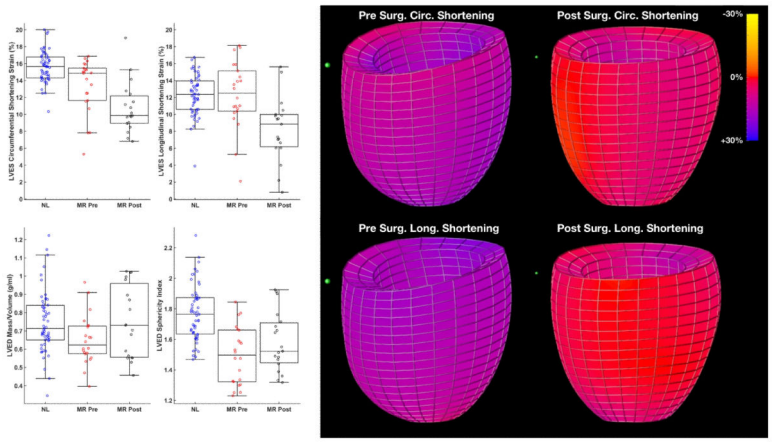

Figure 1. LVED mass/volume, LVED sphericity index and LV circumferential and longitudinal shortening strains in MR patients pre- and six month post-mitral valve (MV) repair with color coded strain maps in MR subject pre- and post-mitral valve repair

Box and whisker plots demonstrate that LVED sphericity index (LVED length/LVED inner diameter) pre- and post-surgery were significantly different from normal controls ($p < 0.0001$ and $p=0.001$ respectively) but did improve post-surgery. LVED mass to volume ratio pre-surgery was significantly different from normal controls ($p=0.0042$) but did improve and did not differ from normal post-surgery ($p=0.0013$). LV longitudinal systolic shortening strains were not different from normal controls before surgery, but were decreased following MV repair vs before surgery ($p=0.0013$) and relative to normal control subjects ($p=0.0020$). The color-coded strain map demonstrates the significant global decrease in circumferential and longitudinal strains in a representative MR patient post mitral valve repair.

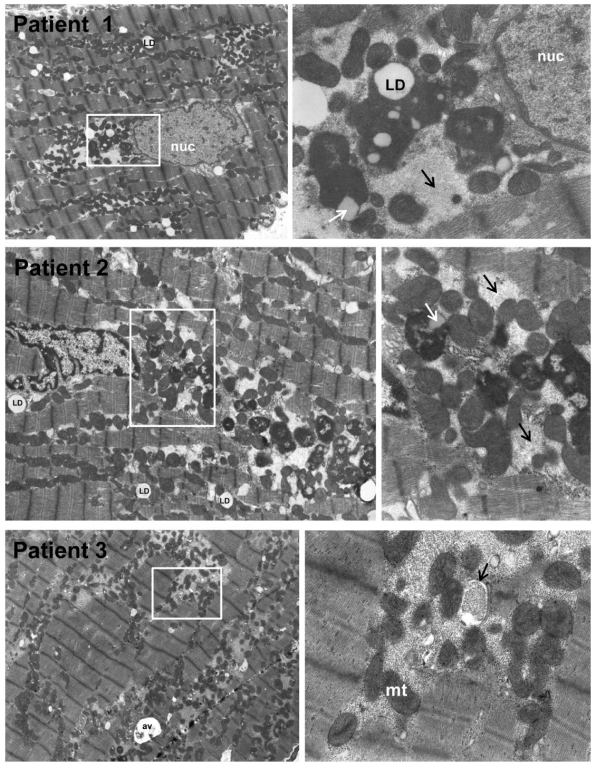

Figure 2. Transmission electron microscopy of LV from 3 patients with MR and LVEF > 60%

In Patients 1-3, 4,500X LV images (left panels) demonstrate extensive myofibrillar breakdown amid mitochondrial (mt) clustering of various small sizes. There is extensive granulofilamentous protein aggregates (right panels, black arrows) representing cytoskeletal and myofibrillar degeneration. In Patients 1 and 2, white boxes (left panels) outline the 16,000X images (right panels) of perinuclear areas with electron dense bodies consistent with lipofuscin also containing lipid droplets (LD) in interfibrillar areas and in electron dense bodies (white arrow Patient 2). Patient 3 demonstrates extensive granulo-filamentous protein aggregates (light gray) in areas of myofibrillar and cytoskeletal degeneration being engulfed by autophagic vacuole (right panel, black arrow in 16,000X image in right panel).

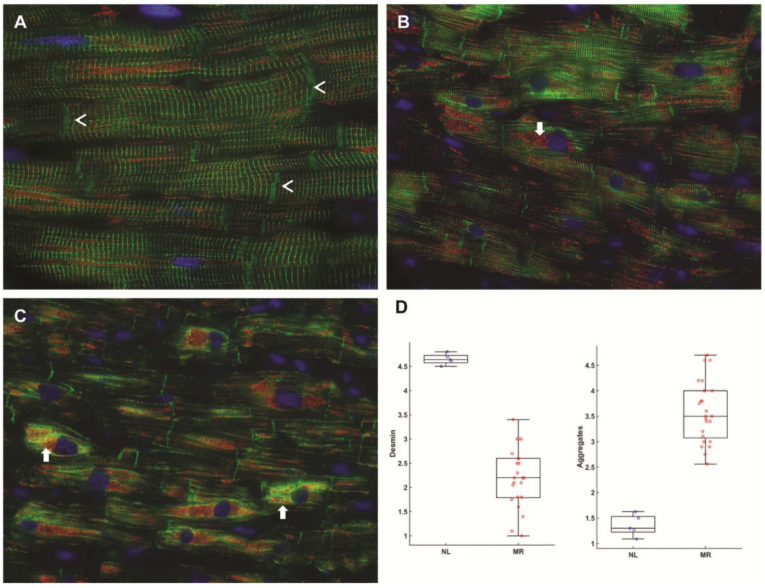

Figure 3. Immunohistochemistry of desmin and VDAC in normal human heart (A) and in patients with MR and LVEF > 60%

Normal LV (A) demonstrates a regular pattern of desmin (green, arrowheads) along Z-lines in between intercalated discs (arrowheads). Co-immunostaining with VDAC (red) show that mitochondria are in linear register in the interfibrillar areas and grouped in perinuclear (DAPI, blue) locations. MR hearts (B and C) demonstrate loss of desmin interspersed with areas of intense desmin staining that co-stains with VDAC (arrows, B and C), especially in the perinuclear areas (arrows). Box-and-whisker plots with the data points superimposed (D) shows the quantitation of desmin loss and aggregate as percent of area of cardiomyocytes. Desmin loss as per cent of cardiomyocytes: Grade 1: 100% loss; Grade 2: 75% loss, 25% intact; Grade 3: 50% loss, 50% intact; Grade 4: 25% loss, 75% intact; and Grade 5: 100% intact. N=22 patients. Desmin staining vs. normal hearts ($p<0.0001$)

Desmin aggregates as percent of cardiomyocytes: Grade 1: no aggregates; Grade 2: 25% aggregates; Grade 3: 50% aggregates; Grade 4: 75%; Grade 5 100% aggregates. N=22 patients. Desmin aggregates vs. normal ($p<0.0001$)

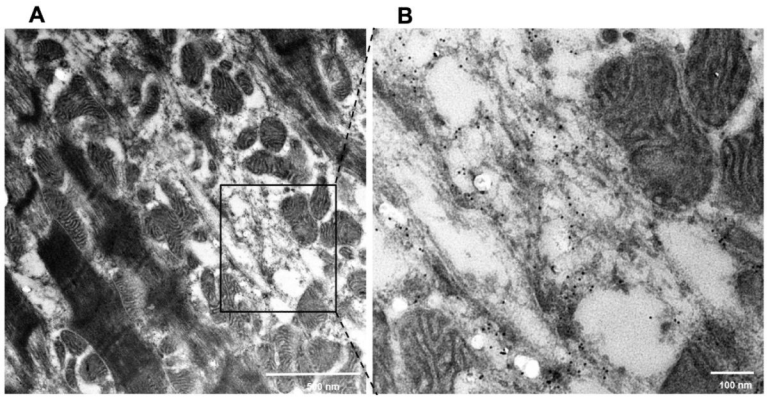

Figure 4. Transmission electron microscopy immunogold labeling for desmin in MR heart

TEM of MR heart of patient with LVEF of 65% demonstrates marked disruption and degradation of the mitochondrial sarcomeric units (left panel) and higher magnification (black box, right panel) of immunogold labeling demonstrates desmin (black dots) in areas of sarcomere/mitchondrial breakdown. Note the desmin in the areas of myofibrillar degradation near the interfibrillar disorganization of mitochondria.

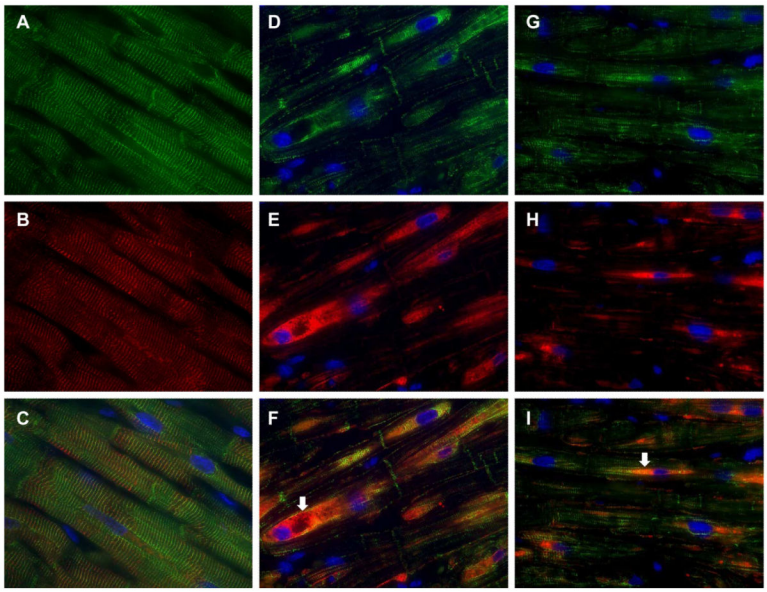

Figure 5. Immunohistochemistry for desmin (green) and αβ-crystallin (red) in MR and normal heart

In the normal heart (A) desmin (green) and α, β-crystallin (red, B) are co-localized to the Z-disc as seen in merged image (C). In MR hearts of patients with LVEF 68% (D-F) and LVEF 62% (G-I) there is extensive desmin loss along with areas of aggregation most prominent in the perinuclear region (DAPI, blue). αβ-crystallin in MR hearts (D-F and G-I) relocates to the perinuclear region (arrows) with desmin aggregates as seen in merged images (F and I).

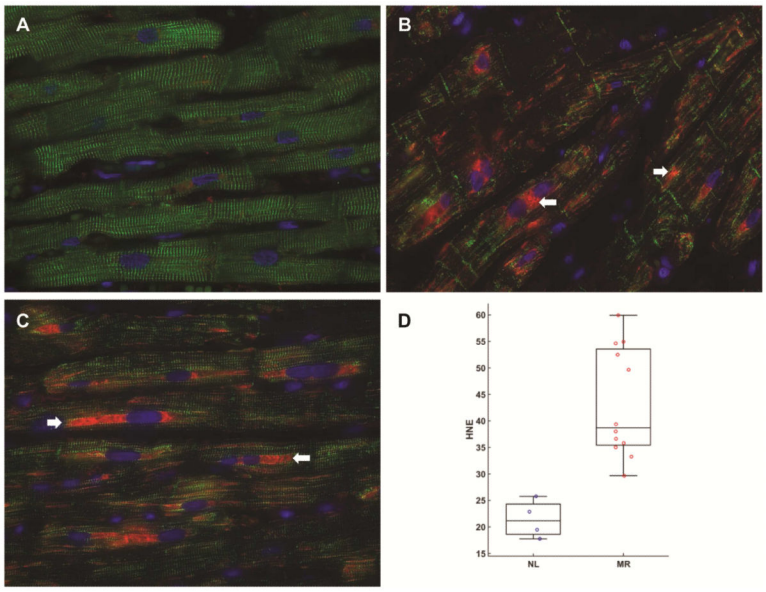

Figure 6. Immunohistochemistry for desmin (green) and 4-hydroxy-2-nonenal (HNE, red) in normal and MR hearts

Normal heart (**A**) has striated pattern of desmin (green) with very little HNE staining (red). In MR hearts (**B, C)** there is extensive desmin loss along with increased HNE staining, especially in the perinuclear areas (arrows) that is increased two-fold in MR hearts in bar graph, measured as HNE intensity as percent area of cardiomyocyte as demonstrated in box and whisker plot (**D**). HNE intensity in MR vs. normal p=0.012)

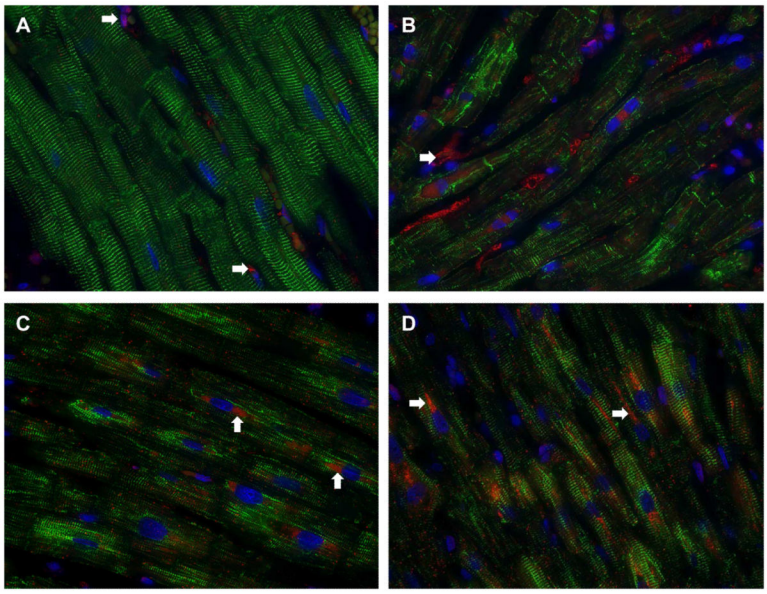

Figure 7. Immunohistochemistry for desmin (green) and catalase (red) in normal and MR hearts

The normal heart (**A**) has the striated desmin with very little catalase staining except in some interstitial cells (**A, arrows**). In three MR hearts (**B-D)** there is extensive desmin loss along with increased catalase staining particularly in the perinuclear regions (**D, arrows**).

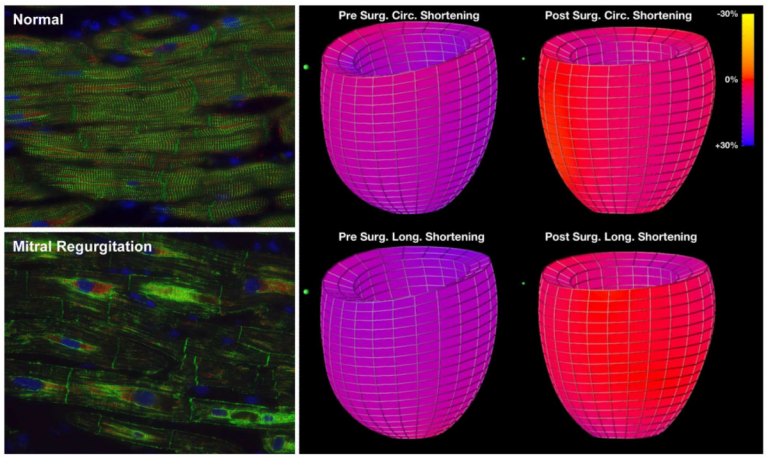

Central Figure.

Breakdown of desmin (green) and aggregation in mitral regurgitation underpins decrease in LV shortening strains below normal (purple to red on color strain map) post-surgery.

Table 1

Demographics, Clinical Characteristics and MRI

Demographic	Mean (Standard Deviation) or Count (%)			
	MR (n=22)		Normal (n=55)	P-value
Gender (Male)	13 (59%)		24 (43%)	0.22
NYHA Class 1	6 (27%)		55 (100%)	NA
Class 2	14 (64%)		0 (0%)	
Class 3	2 (9%)		0 (0%)	
Race (Caucasian)	19 (86%)		39 (71%)	0.15
Age (yrs)	57 (12)		45 (14)	0.0006
Clinical	**MR Pre-surgery (n=22)**	**6 months post-MVR (n=19)**	**Normal (n=55)**	**Main Effect P-value**
BSA (m^2)	1.87 (0.25)	1.84 (0.27)	1.89 (0.24)	0.2143
Heart Rate (BPM)	70 (11)	81 (18)	71 (13)	0.0724
Systolic BP (mmHg)	126 (18)	123 (23)	119 (13)	0.1609
Diastolic BP (mmHg)	74 (7)	77 (10)	74 (10)	0.5190
LVEDD (cm)	6.01 (0.65) vs normal<0.0001 vs post-MVR<0.0001	5.38 (0.75) vs normal =0.0078	5.02 (0.47)	<0.0001
LVESD (cm)	4.17 (0.60) vs normal<0.0001 vs post-MVR ns	4.17 (0.83) vs normal <0.0001	3.52 (0.41)	0.0004
LVEDV (ml)	195 (50) vs normal<0.0001 vs post-MVR =0.0002	152 (45) vs normal =0.0012	127 (27)	0.0001
LVESV (ml)	67 (20) vs normal<0.0001 vs post-MVR ns	74 (33) vs normal<0.0001	45 (14)	0.0002
LVEF (%)	65 (7) vs normal ns vs post-MVR <0.0001	52 (9) vs normal <0.0001	65 (6)	0.0002
LV circ short (%)	13.4 (3.2) vs normal=0.0145 vs post-MVR =0.001	10.8 (3.0) vs normal <.0001	15.6 (1.8)	0.0002
LV long short (%)	12.3 (4.0) vs normal ns vs post-MVR =0.0013	8.3 (3.7) vs normal =0.002	12.3 (2.4)	0.0052
LVED sphericity	1.5 (0.2) vs normal<0.0001 vs post-MVR=0.015	1.6 (0.2) vs normal =0.001	1.8 (0.2)	0.0005
LVED mass/vol	0.65 (0.1) vs normal=0.0042 vs post-MVR =0.0013	0.75 (0.2) vs normal ns	0.75 (0.2)	0.0057